

Linking bacterial and archaeal community dynamics to related hydrological, geochemical and environmental characteristics between surface water and groundwater in a karstic estuary

Xiaogang Chen^{1,2}, Qi Ye^{1*}, Jinzhou Du¹, Neven Cukrov³, Nuša Cukrov³, Yan Zhang², Ling Li², Jing Zhang¹

¹ State Key Laboratory of Estuarine and Coastal Research, East China Normal University, Shanghai 200241, China

² Key Laboratory of Coastal Environment and Resources of Zhejiang Province, School of Engineering, Westlake University, Hangzhou 310024, China

³ Division for Marine and Environmental Research, Ruđer Bošković Institute, Zagreb 10000, Croatia

Received 27 October 2022; accepted 11 March 2023

© Chinese Society for Oceanography and Springer-Verlag GmbH Germany, part of Springer Nature 2023

Abstract

Subterranean estuaries (STEs) are characterized by the mixing of terrestrial fresh groundwater and seawater in coastal aquifers. Although microorganisms are important components of coastal groundwater ecosystems and play critical roles in biogeochemical transformations in STEs, limited information is available about how their community dynamics interact with hydrological, geochemical and environmental characteristics in STEs. Here, we studied bacterial and archaeal diversities and distributions with 16S rRNA-based Illumina MiSeq sequencing technology between surface water and groundwater in a karstic STE. Principal-coordinate analysis found that the bacterial and archaeal communities in the areas where algal blooms occurred were significantly separated from those in other stations without algal bloom occurrence. Canonical correspondence analysis showed that nutrients and salinity can explain the patterns of bacterial and archaeal community dynamics. The results suggest that hydrological, geochemical and environmental characteristics between surface water and groundwater likely control the bacterial and archaeal diversities and distributions in STEs. Furthermore, we found that some key species can utilize terrestrial pollutants such as nitrate and ammonia in STEs, indicating that these species (e.g., *Nitrosopumilus maritimus*, *Limnohabitans parvus* and *Simplicispira limi*) may be excellent candidates for *in situ* degradation/remediation of coastal groundwater contaminations concerned with the nitrate and ammonia. Overall, this study reveals the coupling relationship between the microbial communities and hydrochemical environments in STEs, and provides a perspective of *in situ* degradation/remediation for coastal groundwater quality management.

Key words: submarine groundwater discharge, surface water and groundwater interaction, algal bloom, microbial ecology, nutrient biogeochemistry, ammonia-oxidizing archaea, nitrate-utilizing bacteria, Krka River Estuary

Citation: Chen Xiaogang, Ye Qi, Du Jinzhou, Cukrov Neven, Cukrov Nuša, Zhang Yan, Li Ling, Zhang Jing. 2023. Linking bacterial and archaeal community dynamics to related hydrological, geochemical and environmental characteristics between surface water and groundwater in a karstic estuary. Acta Oceanologica Sinica, 42(8): 158–170, doi: 10.1007/s13131-023-2185-7

1 Introduction

The subterranean estuary (STE) is a reactive mixing zone between fresh groundwater and recirculated seawater (Moore, 1999; Rocha et al., 2021), which is considered to be a significant contributor of bacteria (Boehm et al., 2004; Knee et al., 2008; Ruiz-González et al., 2021) and biogenic elements such as nutrients (Cai et al., 2015; Wang et al., 2018; Chen et al., 2021a; Santos et al., 2021; Zhao et al., 2021), carbon (Liu et al., 2014; Wang et al., 2014; Chen et al., 2018b, 2022; Yau et al., 2022), metals (Wang et al., 2019; Mayfield et al., 2021; Zhong et al., 2022) and greenhouse gases (Chen et al., 2021b, 2023; Reading et al., 2021; Zhu et al., 2022) to coastal waters. Biogeochemical reactions in STEs are often mediated by microorganisms, which can modify the chemical composition of submarine groundwater (Santoro et al., 2008;

Adyasari et al., 2019, 2020; Chen et al., 2019, 2020b; Zhang et al., 2021). For example, bacterial processes contribute to the nitrate removal and dissolved inorganic carbon (DIC) addition in a sandy STE (Chen et al., 2020b). However, compared with inland groundwater, the microbial dimension of submarine groundwater discharge (SGD) remains poorly understood (Archana et al., 2021; Ruiz-González et al., 2021).

As the most abundant and diverse group of life on the Earth, microbial communities have an integral function and play a pivotal role in biogeochemical cycling to marine ecosystem, and that has no exception for SGD (DeLong and Karl, 2005; Ye et al., 2016; Adyasari et al., 2020). Several studies of microbial communities in STEs were reported and novel insights involve using 16S rRNA (Ye et al., 2016; Adyasari et al., 2019, 2020; Chen et al.,

Foundation item: The National Key R&D Program of China under contract No. 2022YFE0209300; the National Natural Science Foundation of China under contract No. 42006152; the Zhejiang Provincial Natural Science Foundation of China under contract No. LQ21D060005; the 111 Project under contract No. BP0820020.

*Corresponding author, E-mail: qye@sklec.ecnu.edu.cn

2019, 2020b; Wu et al., 2021) and functional genes (Santoro et al., 2006, 2008) to reveal microbial communities in STE systems. Large amounts of nutrients, carbon and greenhouse gases entering the coastal waters via SGD may lead to outbreaks of eutrophication (Hwang et al., 2005), algal blooms (Chen et al., 2020a; Zhao et al., 2021), deoxygenation (Guo et al., 2020) and localized coastal acidification (Wang et al., 2014; Cardenas et al., 2020). However, the coupling of microbial communities and environmental problems (e.g., red tides) in SGD is less reported, which limits the understanding on the biogeochemical cycle and environmental management in STE ecosystems.

The Krka River Estuary is a salt-wedge, highly stratified estuary, located in the central part of the eastern Adriatic coast (Croatia) (Liu et al., 2019). As in other Mediterranean karstic shorelines, anchialine environments are common in the Krka River Estuary. These types of environments are characterized by highly stratified water column and connection with the open sea, usually through the karst carbonate rock, showing noticeable marine as well as terrestrial influences (Žic et al., 2008; Kwokal et al., 2014). Previous ^{222}Rn mass balance has shown that anchialine caves or springs can deliver point-source, nitrogen enriched groundwater with high N/P molar ratio to the coastal waters in the Krka River Estuary, which trigger and sustain red tide outbreaks (Chen et al., 2020a). Therefore, these anchialine caves or springs are reasonable and representative groundwater end-members in the Krka River Estuary (Liu et al., 2019; Chen et al., 2020a). As one kind of the important STEs, anchialine system has complex and variable hydrological, geochemical and environmental characteristics in the Krka River Estuary and provides direct access to the aquifer source (Bishop et al., 2015). However, the coupling relationship between these complex characteristics and bacterial and archaeal community dynamics is still poorly understood despite their potentially important implications for nutrient and carbon cycling.

Here, we hypothesize that bacterial and archaeal community dynamics interact with the hydrological, geochemical and environmental characteristics in STEs. We investigated the bacterial

and archaeal diversities by utilizing 16S rRNA-based Illumina MiSeq sequencing technology and related salinity, ^{222}Rn (a groundwater tracer), nutrients and carbon in submarine groundwater (including anchialine caves and springs) and surface water along the Krka River Estuary. This study aims to (1) explore coupling relationship between bacterial and archaeal community dynamics and related hydrological, geochemical and environmental characteristics (e.g., algal blooms) in karstic STEs, and (2) provide insights on the mechanisms of controlling the input or removal of terrigenous materials affected by bacterial and archaeal communities in STE ecosystems, and (3) find the related key candidates for bioremediation in the polluted SGD.

2 Materials and methods

2.1 Study area

The Krka River Estuary is an oligotrophic stratified karstic estuary, which is sensitive to inputs of external substances such as nutrients and carbon (Liu et al., 2019; Chen et al., 2020a). The mean water flow of the Krka River is between $40\text{ m}^3/\text{s}$ and $60\text{ m}^3/\text{s}$ (Bonacci et al., 2006). Algal blooms were observed in the estuary and showed obvious seasonal outbreaks (Chen et al., 2020a). The Krka River Estuary has a micro-tidal nature (tidal range: 0.2–0.5 m) with strong stratification. The area is characterized by mild, wet winters and warm, dry summers, with an annual average precipitation of $\sim 900\text{ mm}$ (http://klima.hr/klima_arhiva.php).

2.2 Sample collection and measurements of physico-chemical parameters

In this study, seven bacterial and archaeal samples (anchialine cave, spring and surface water) were collected along the Krka River Estuary in April, 2016 (Fig. 1). Each sample ($\sim 5\text{ L}$) was collected on a $0.22\text{ }\mu\text{m}$ pore size polycarbonate filter (Nuclepore Track-Etched Membrane, Whatman, UK), then placed in a sterile 1.5 mL microcentrifuge tube and was immediately placed and kept in the fridge ($-20\text{ }^\circ\text{C}$). ^{222}Rn samples were collected in 250 mL glass bottles and analyzed by RAD7 detector immediately. Nutri-

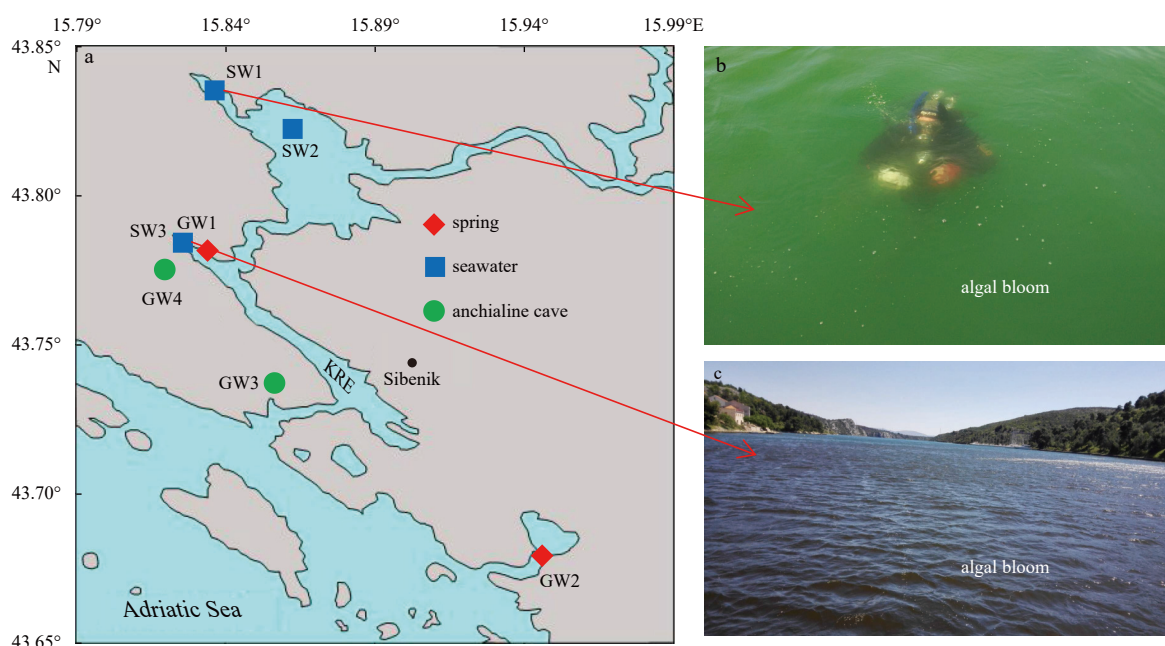


Fig. 1. Study site location and sampling stations (a) in the Krka River Estuary (KRE). Algal bloom occurred at surface water stations SW1 (b) and SW3 (c) during sampling (April 2016). SW: seawater; GW: groundwater.

ent and carbon samples were collected with polyethylene bottles, then stored at -20°C and kept away from light. The nutrients (NO_2^- , NO_3^- , NH_4^+ and PO_4^{3-}) were analyzed using the method of [Strickland and Parsons \(1972\)](#). The DIC and dissolved organic carbon (DOC) were determined using TOC-V Analyser (Shimadzu®, Japan). Salinity and temperature were measured directly in the field using a multi parametric probe (Hach Lange HQ40D, USA).

2.3 DNA extraction, polymerase chain reaction (PCR), and sequencing

Total DNA was extracted from each filter using a MoBio PowerWater® DNA Isolation Kit (MOBIO Laboratories, Carlsbad, USA). DNA concentration and purity were quantified spectrophotometrically with NanoDrop ND2000 (USA).

To decrease PCR bias, minimum numbers of PCR cycles were performed and three independent PCR mixtures were pooled for each sample. The bacterial 16S rRNA genes were amplified using the specific barcoded universal primer pairs 515F (5'-GTG-CAGCMGCCGCGG-3') and 907R (5'-CCGCAATTCMTTTRAGT-TT-3') spanning the V4-V5 hypervariable regions ([Xiong et al., 2012](#)). Cycling conditions were an initial denaturation at 95°C for 2 min, 25 cycles of 95°C for 30 s, 55°C for 30 s, 72°C for 30 s and a final 5-min extension at 72°C . Meanwhile, the archaeal 16S rRNA genes were amplified using specific barcoded universal primer pairs 524F10extF (5'-TGYCAGCCGCCGCGGTAA-3') and Arch958RmodR (5'-YCCGGCGTTGAVTCCAATT-3') ([Pires et al., 2012](#)) using the following amplification conditions: 3 min at 95°C , followed by 35 cycles with 30 s at 95°C , 30 s at 55°C , 45 s at 72°C , and a final extension period of 10 min at 72°C . PCR products from each tagged primer were purified using the AxyPreDNA gel extraction kit (Axygen Biosciences, USA) and then quantified by QuantiFluor™-ST (Promega, USA). Finally, reaction mixtures were pooled in equimolar ratios and paired-end reads were generated on an Illumina MiSeq PE250 (Majorbio Bio-Pharm Technology Co., Ltd., China, <http://www.majorbio.bion.com.cn/>).

Raw Illumina FASTQ files were demultiplexed, quality-filtered, and analyzed using Quantitative Insights into Microbial Ecology (QIIME) (version 1.9.1) ([Caporaso et al., 2010](#)) as the criteria described previously ([Chen et al., 2020b](#)). Reads that could not be assembled were discarded. The UCHIME algorithm in the USEARCH platform was used to detect and remove chimeric sequences, which performs both de novo chimera and reference-based detection ([Edgar et al., 2011](#)). Operational taxonomic units

(OTUs) with 97% similarity cutoff were clustered using UPARSE ([Edgar, 2013](#)). The OTU Cluster was used to determine OTU abundances. The number of reads from each sample that was assigned to each OTU was generated as an "OTU table" by using the Usearch_global command. The sequence reads of all samples were randomly resampled to the smallest sample size. The taxonomic assignment of representative OTU sequences was analyzed by the Ribosomal Database Project Classifier (version 2.11, <http://rdp.cme.msu.edu/>).

2.4 Phylogenetic analyses

The sequences of the representative OTUs obtained in this study were compared to those in the National Center for Biotechnology Information (NCBI) nucleotide database by using Basic Local Alignment Search Tool (BLAST, [Altschul et al., 1997](#)) searching. The closest sequences and selected reference sequences were downloaded and aligned using Clustal W. Phylogenetic trees were generated in MEGA7 using the neighbor-joining method with a bootstrap test of 1 000 replicates and maximum composite likelihood model ([Tamura et al., 2013](#)).

2.5 Statistical analyses

Alpha diversity metrics and coverage were measured and calculated using the Mothur Program ([Schloss et al., 2009](#)). Hierarchical clustering of the samples was performed with the complete method using the function hclust of stats package in R (R Development Core Team, 2013; <http://www.R-project.org/>). Principal-coordinate analyses (PCoA) were performed to show if distinct separations in bacterial or archaeal community structures were present between groundwater and surface water. To determine which environmental variables best explained patterns of bacterial and archaeal communities, canonical correspondence analysis (CCA) was applied ([ter Braak, 1986](#)).

3 Results and discussion

3.1 Site description and environmental characteristics

Surface water and submarine groundwater (spring and anchialine cave water) samples were collected in this study ([Fig. 1](#)). Groundwater (including spring water and anchialine cave water) had lower salinity and higher nutrient concentrations than surface water ([Table 1](#)). Based on this, seven samples were separated into two groups: Group G included 2 spring samples (GW1 and GW2) and 2 anchialine cave samples (GW3 and GW4), and

Table 1. The site descriptions and physico-chemical parameters

| Station | SW1 | SW2 | SW3 | GW1 | GW2 | GW3 | GW4 |
|--|-----------------------|-----------------------------------|---|-----------------------------------|-----------------|---|-----------------|
| Longitude | 15.834 4°E | 15.864 4°E | 15.827 6°E | 15.832 2°E | 15.949 2°E | 15.860 1°E | 15.810 6°E |
| Latitude | 43.837 0°N | 43.816 6°N | 43.782 0°N | 43.780 7°N | 43.678 1°N | 43.737 3°N | 43.777 5°N |
| Water type | surface water | surface water | surface water | spring | spring | anchialine cave | anchialine cave |
| Characteristics of sampling site | algal bloom happening | located in the center of the lake | near the Station GW1; algal bloom happening | near the village; in the open air | near the lagoon | natural cave; smelly water; water hypoxia (DO: 0.62 mg/L) | natural cave |
| Temperature/ $^{\circ}\text{C}$ | 13.5 | 15.0 | ND | 14.7 | 15.3 | ND | ND |
| Salinity | 3.1 | 6.4 | 9.2 | 1.1 | 3.4 | 0.7 | 0.8 |
| $^{222}\text{Rn}/(\text{Bq}\cdot\text{m}^{-3})$ | 918 | 54 | 215 | 1 748 | ND | 881 | 681 |
| $\text{NO}_3^-/(\mu\text{mol}\cdot\text{L}^{-1})$ | 178.01 | 18.50 | 42.51 | 178.57 | 79.66 | 14.22 | ND |
| $\text{NO}_2^-/(\mu\text{mol}\cdot\text{L}^{-1})$ | 0.67 | 0.32 | 0.26 | 0.03 | 0.03 | 0.12 | ND |
| $\text{NH}_4^+/(\mu\text{mol}\cdot\text{L}^{-1})$ | 2.79 | 1.87 | 1.00 | 1.31 | 0.50 | 2.14 | ND |
| $\text{PO}_4^{3-}/(\mu\text{mol}\cdot\text{L}^{-1})$ | 0.91 | 0.20 | 0.16 | 0.95 | 0.23 | 2.67 | ND |
| DIC/($\text{mg}\cdot\text{L}^{-1}$) | 65.62 | 50.77 | ND | 61.10 | ND | ND | ND |
| DOC/($\text{mg}\cdot\text{L}^{-1}$) | 1.32 | 0.93 | ND | 0.68 | ND | ND | ND |

Note: ND represents not determined.

the salinity of Group G ranged from 0.7 to 3.4 with a mean of 1.5; Group S included three surface water samples (SW1, SW2 and SW3) with relatively higher salinity, which ranged from 3.1 to 9.2 with a mean of 6.2. Group S had mean values of 396 Bq/m³, 79.67 μmol/L and 0.42 μmol/L for ²²²Rn, NO₃⁻ and PO₄³⁻. However, Group G had higher mean values of 1 103 Bq/m³, 90.82 μmol/L and 1.28 μmol/L for ²²²Rn, NO₃⁻ and PO₄³⁻, respectively. NO₂⁻ concentrations ranged from 0.03 μmol/L to 0.12 μmol/L in Group G, lower than those in Group S (0.26–0.67 μmol/L). Mean NH₄⁺ concentration in Group S (1.89 μmol/L) was slightly higher than that in Group G (1.32 μmol/L). There was no distinct pattern of DIC concentration between Group G and Group S. DOC concentration in Group S (1.13 mg/L) was higher than that in Group G (0.68 mg/L). The temperature values (13.5–15.3°C) were relatively constant at all sites.

For surface water, the ²²²Rn and NO₃⁻ concentrations of Stations SW1 and SW3 were significantly higher than those of Station SW2, indicating that SW1 and SW3 were significantly affected by high concentrations of groundwater ²²²Rn and NO₃⁻. Algal blooms occurred at surface water stations SW1 and SW3 during the sampling period, which further indicates that groundwater provides the major nutrients such as NO₃⁻ for algae blooms due to the lack of other significant nutrient sources in the Krka River Estuary (Chen et al., 2020a).

3.2 Microbial diversity and distribution in groundwater-surface water interaction

Totally seven bacterial and archaeal samples were analyzed by using high throughput sequencing, and a total of 195 417 high-quality bacterial V4-V5 Illumina sequences and 139 040 high-quality archaeal V4-V5 Illumina sequences were retrieved. There were 2 830 bacterial OTUs and 680 archaeal OTUs in the complete OTU data set at the 97% similarity cutoff. Good coverage was 99.5%–99.9% for all samples after subsampling (Table 2). Richness index (including ACE and Chao) of bacterial community ranged from 332 to 398 in surface water, significantly lower than those in groundwater (434–797). There was no significant difference in archaeal richness between surface water (59–138) and groundwater (81–136). Bacterial and archaeal diversities (e.g., Shannon index) showed variability in both surface water and submarine groundwater (Table 2).

PCoA analyses showed that both the bacterial and archaeal communities in the areas where algal blooms occurred (i.e., Stations SW1 and SW3) were significantly separated from those in other stations along the first axis explaining 21.2% and 50.3% of the variations (Fig. 2), respectively, which may indicate that the spatial niche partitioning of the bacterial and archaeal communities at Stations SW1 and SW3 and related ecological functions were different from other stations (Chen et al., 2019).

Taxonomic distributions showed that there were no significant variations in the proportion of Illumina sequences among the bacterial samples, but there were some differences among archaeal samples (Fig. 3). For all bacterial samples, *Gammaproteobacteria* (29.0%–78.8%), *Alphaproteobacteria* (3.6%–33.5%) and *Bacteroidia* (0.3%–27.8%) were the three main bacterial taxa. *Cyanobacteriia* and *Actinobacteria* also accounted for a larger proportion at surface water stations SW1 (13.7%) and SW3 (17.2%), respectively. For archaeal samples, the most dominant genus at spring water stations GW1 (51.7%) and GW2 (59.7%) was *Candidatus Nitrosopumilus*. The genus of *Candidatus Nitrosoarchaeum* was found abundantly at anchialine cave stations GW3 (97.7%) and GW4 (54.1%) and surface water station SW2 (91.3%), and *Candidatus Nitrosoarchaeum* was also the second dominant genus at spring water stations GW1 (21.1%) and GW2 (12.6%).

Table 2. High throughput sequence information and diversity and richness estimators of bacterial and archaeal communities in groundwater (spring and anchialine cave water) and surface water

| Station | Optimized sequence | Observed OTU | ACE | Chao | Shannon index | Coverage |
|-----------------|--------------------|--------------|-----|------|---------------|----------|
| Bacteria | | | | | | |
| SW1 | 31 351 | 317 | 384 | 398 | 3.03 | 0.997 |
| SW2 | 21 363 | 278 | 342 | 332 | 3.50 | 0.997 |
| SW3 | 32 245 | 299 | 381 | 377 | 2.11 | 0.997 |
| GW1 | 23 958 | 329 | 455 | 434 | 2.78 | 0.995 |
| GW2 | 28 391 | 715 | 780 | 797 | 4.72 | 0.996 |
| GW3 | 28 485 | 401 | 473 | 482 | 3.71 | 0.997 |
| GW4 | 29 624 | 491 | 579 | 592 | 4.13 | 0.996 |
| Archaea | | | | | | |
| SW1 | 33 311 | 138 | 138 | 138 | 2.66 | 0.999 |
| SW2 | 33 556 | 53 | 58 | 59 | 0.55 | 0.999 |
| SW3 | 31 043 | 105 | 106 | 105 | 2.17 | 0.999 |
| GW1 | 31 363 | 115 | 125 | 132 | 1.85 | 0.999 |
| GW2 | 35 450 | 134 | 138 | 136 | 1.70 | 0.999 |
| GW3 | 41 968 | 55 | 68 | 81 | 0.17 | 0.999 |
| GW4 | 32 349 | 80 | 85 | 86 | 1.87 | 0.999 |

Note: OTU: operational taxonomic units; ACE: abundance-based coverage estimator; Chao: Chao1 species richness.

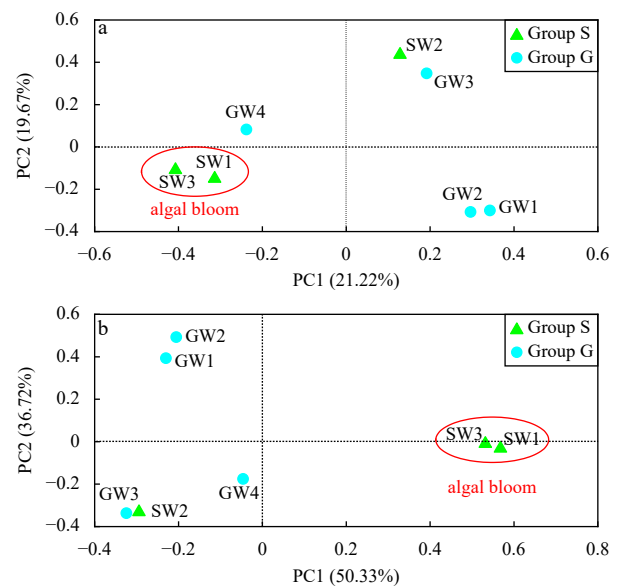


Fig. 2. The principal-coordinate analyses (PCoA) analyses on operational taxonomic units (OTU) levels of bacterial (a) and archaeal (b) communities in surface water (green triangles) and submarine groundwater (cyan dots). Notice the algal bloom happening at Stations SW1 and SW3.

However, the genera of *Candidatus Nitrosopumilus* and *Candidatus Nitrosoarchaeum* were seldom detected at surface water stations SW1 (<1%) and SW3 (0.5%–2.2%) where algal blooms occurred. Crenarchaeotic Group archaea was the most abundant group at surface water stations SW1 and SW3, which further indicates that Crenarchaeotic Group archaea may be related to algal bloom outbreaks at these stations.

In previous studies, *Proteobacteria* dominated all bacterial groundwater samples, which belongs to *Alphaproteobacteria*, *Betaproteobacteria* and *Gammaproteobacteria* at the genus level (Archana et al., 2021). In our study, the microbial diversity and distribution in groundwater samples were consistent with these

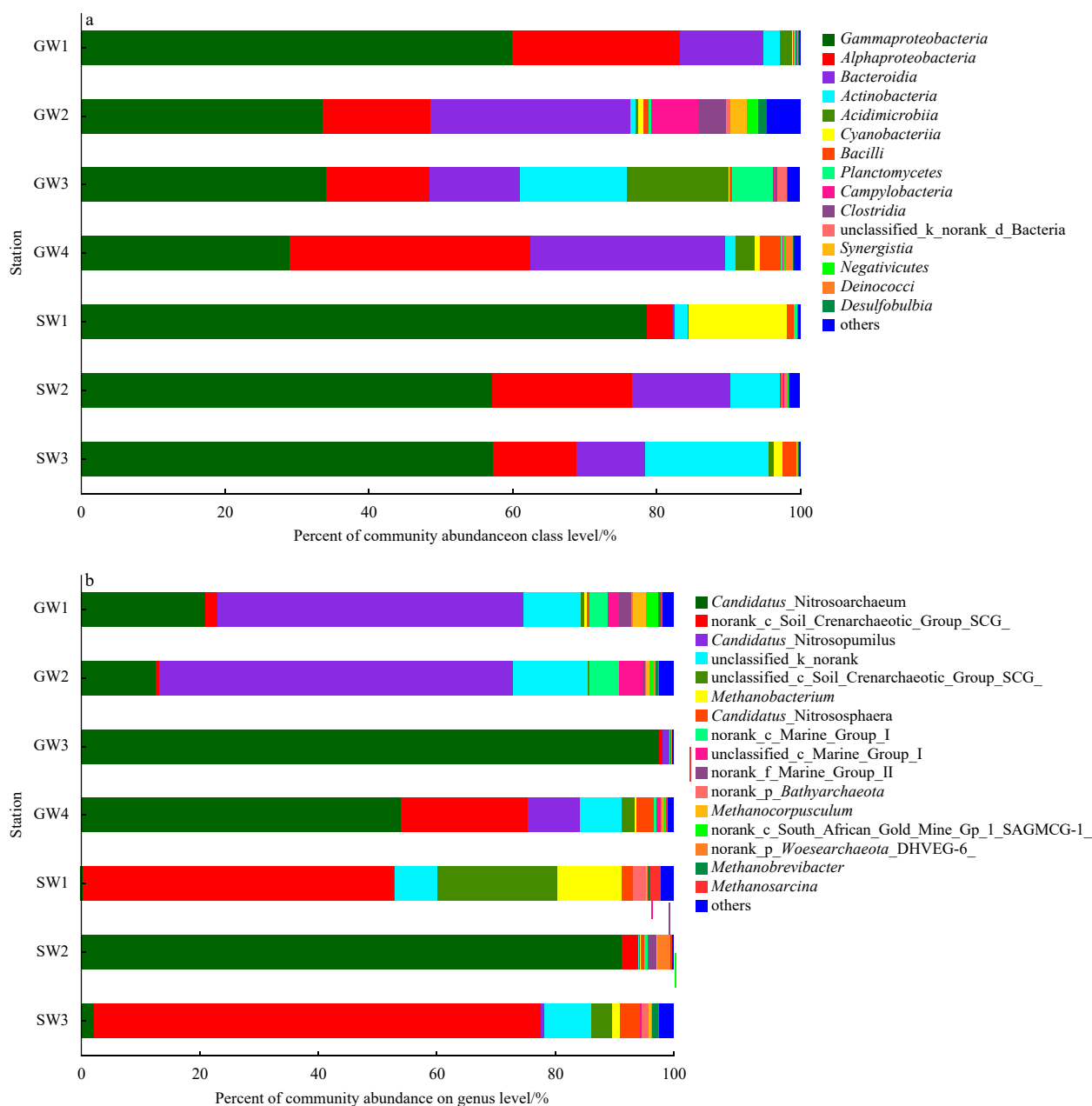


Fig. 3. The relative composition of bacterial (a) and archaeal (b) taxa across all samples. Bacterial and archaeal taxa represented by less than 1% reads are pooled as “others”.

previous results (Fig. 3). Although previous data on groundwater archaea are limited, these archaea results indicate that *Euryarchaeota*, *Crenarchaeota*, *Bathyarchaeota* and *Thaumarchaeota* were widely distributed in groundwater samples (Archana et al., 2021), but the dominant groundwater archaea in this study was *Candidatus Nitrosopumilus* (Fig. 3).

3.3 Ecological niches of microbial community in groundwater-surface water interaction

Surface water and groundwater interactions in coastal areas are active mixing zones with characteristic ecological functions (Lee et al., 2017). The dominant bacterial and archaeal communities were significantly different in submarine groundwater and surface water (Fig. 4). For example, the dominant bacterial communities in groundwater samples were *Limnohabitans* and *Psychrobacter* while that in the surface water were *Flavobacteri-*

um and *Rickettsiella*. The results suggest that the environmental differences between the subterranean and surface estuaries may affect the microbial diversity and distribution, which in turn affect their biogeochemical and ecological functions.

Previous studies emphasized that microbes participate in the carbon and nutrient cycling in STEs and determined the chemistry of the groundwater reaching the ocean (Chen et al., 2019, 2020b; Ruiz-González et al., 2021). In this study, the neighbor-joining method was adopted to construct the bacterial phylogenetic tree (Fig. 5). The sequences of OTU32B were frequently obtained from groundwater (proportion of OTUs: 1.3%–45.5%) and exhibited 99.0% similarity with *Limnohabitans parvus* strain II-B4 (NR_125542), which may serve as ammonium oxidizer (Kasalický et al., 2010). Some OTU sequences such as OTU515B, OTU593B, OTU352B, OTU193B and OTU672B were detected in some groundwater stations (proportion of OTUs: 3.2%–6.5%),

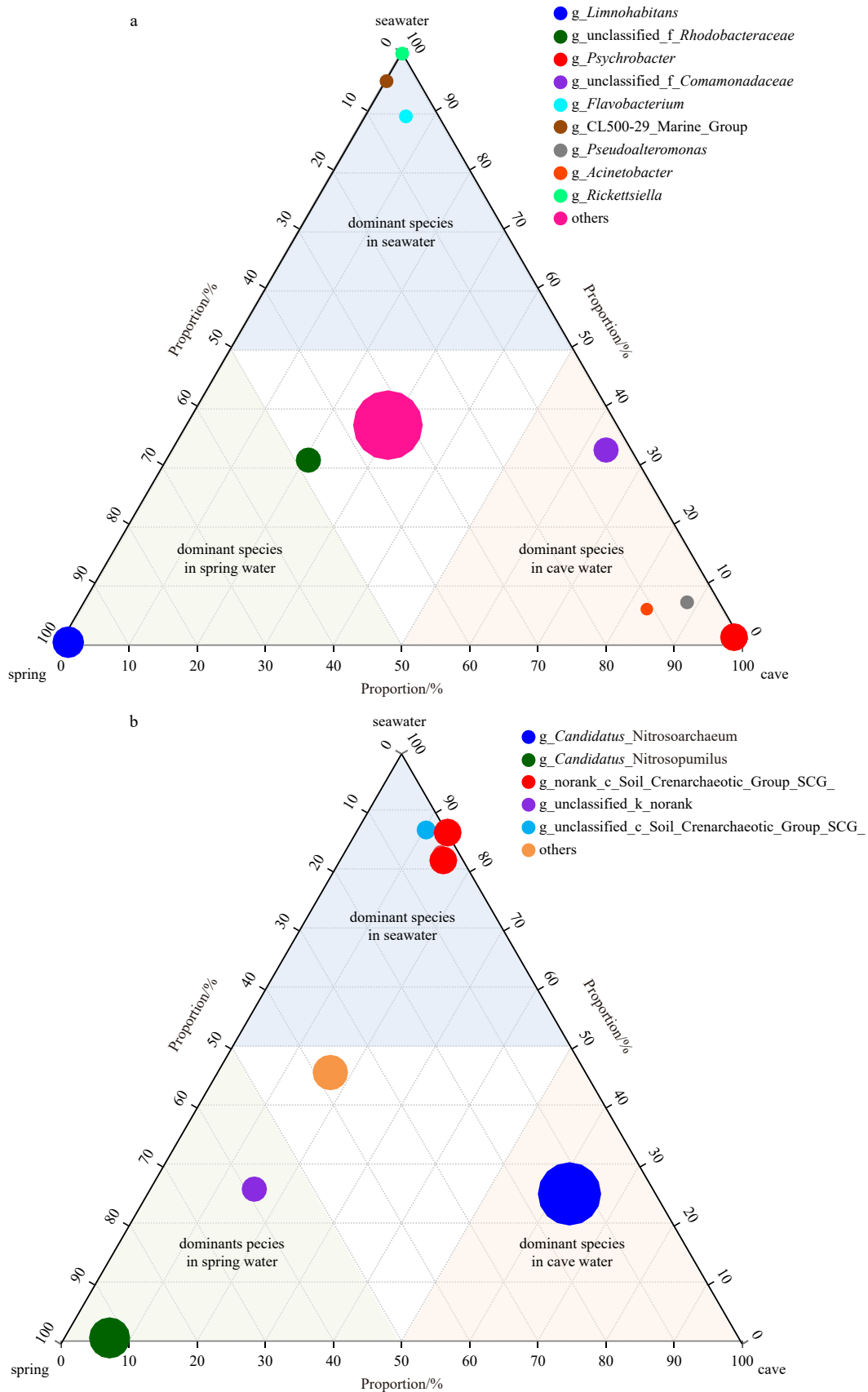


Fig. 4. Ternary diagram illustrating the dominant bacterial (a) and archaeal (b) communities in surface water, spring water and anchialine cave water.

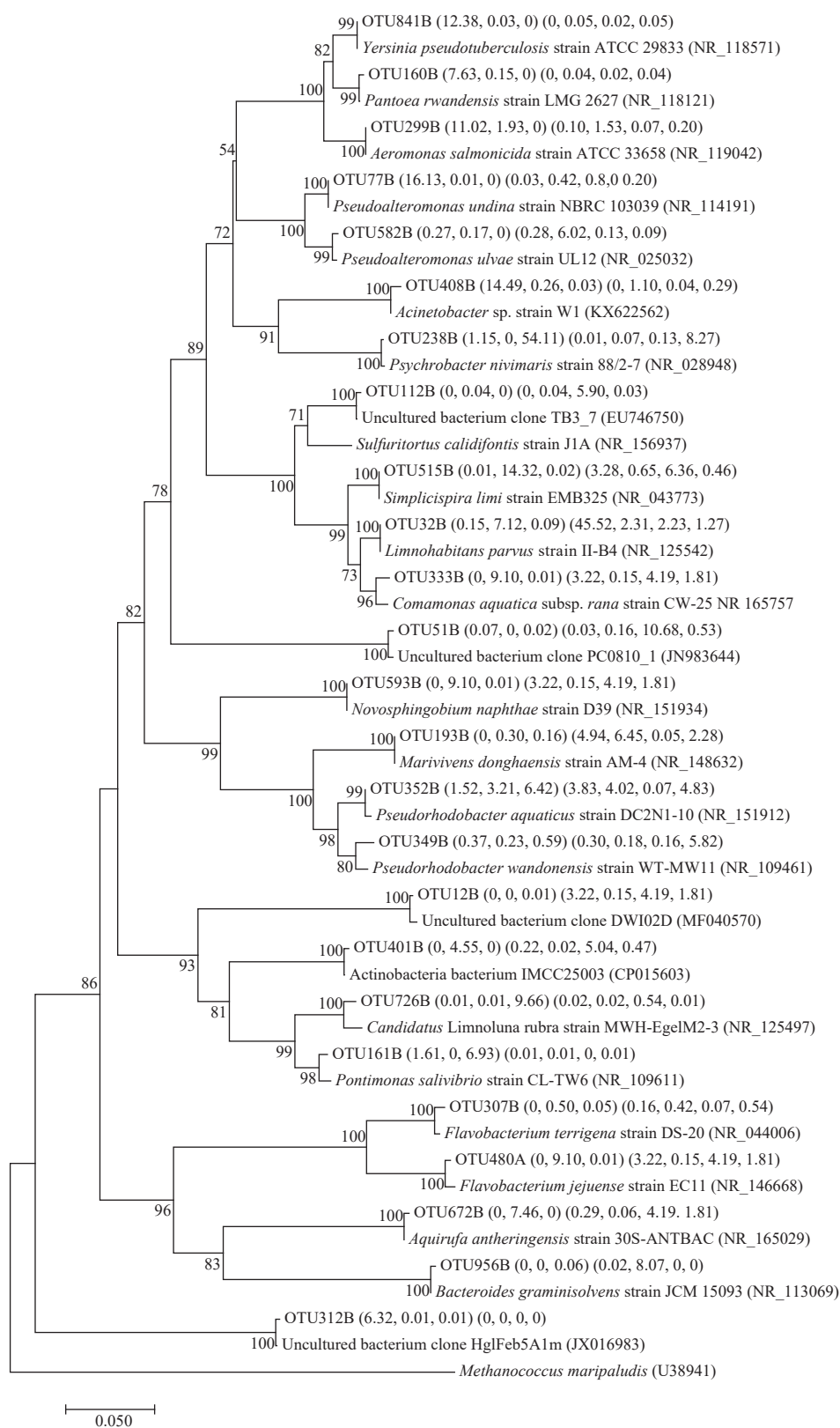


Fig. 5. Neighbor-joining tree showing phylogenetic relationships among the major bacterial operational taxonomic units (OTUs) and reference 16S rRNA gene sequences retrieved from the National Center for Biotechnology Information (NCBI) GenBank. These OTUs were those that ranked top five reads from at least a single sample. The scale bar represents the estimated number of nucleotide changes per sequence position. Percentage on nodes refer to the percentage of recovery from 1 000 bootstrap resamplings. Only values larger than 50% are shown. The numbers in parentheses indicate the percentage composition of reads in each station in the following order: (SW1, SW2, SW3) (GW1, GW2, GW3, GW4). *Methanococcus maripaludis* (U38941) was used as the outgroup.

which had 99.5%–100% matches to *Simplicispira limi* strain EMB325 (NR_043773) (Lu et al., 2007), *Novosphingobium naphthae* strain D39 (NR_151934) (Chaudhary and Kim, 2016), *Pseudorhodobacter aquaticus* strain DC2N1-10 (NR_151912) (Li et al., 2016), *Marivivens donghaensis* strain AM-4 (NR_148632) (Park et al., 2016) and *Aquirufa antheringensis* strain 30S-ANTBAC (NR_165029) (Pitt et al., 2019), respectively. These strains can strongly reduce nitrate through nitrate reduction. These OTU se-

quences (except OTU193B) were also frequently found in surface water, indicating the connectivity in groundwater-surface water interaction.

In the archaeal analysis, neighbor-joining tree was used to show phylogenetic relationships among the representative OTUs (Fig. 6). The sequences of OTU199A were frequently obtained from groundwater (proportion of OTUs: 1.1%–67.0%) but rarely in surface water (proportion of OTUs: 0–0.5%), and showed >99%

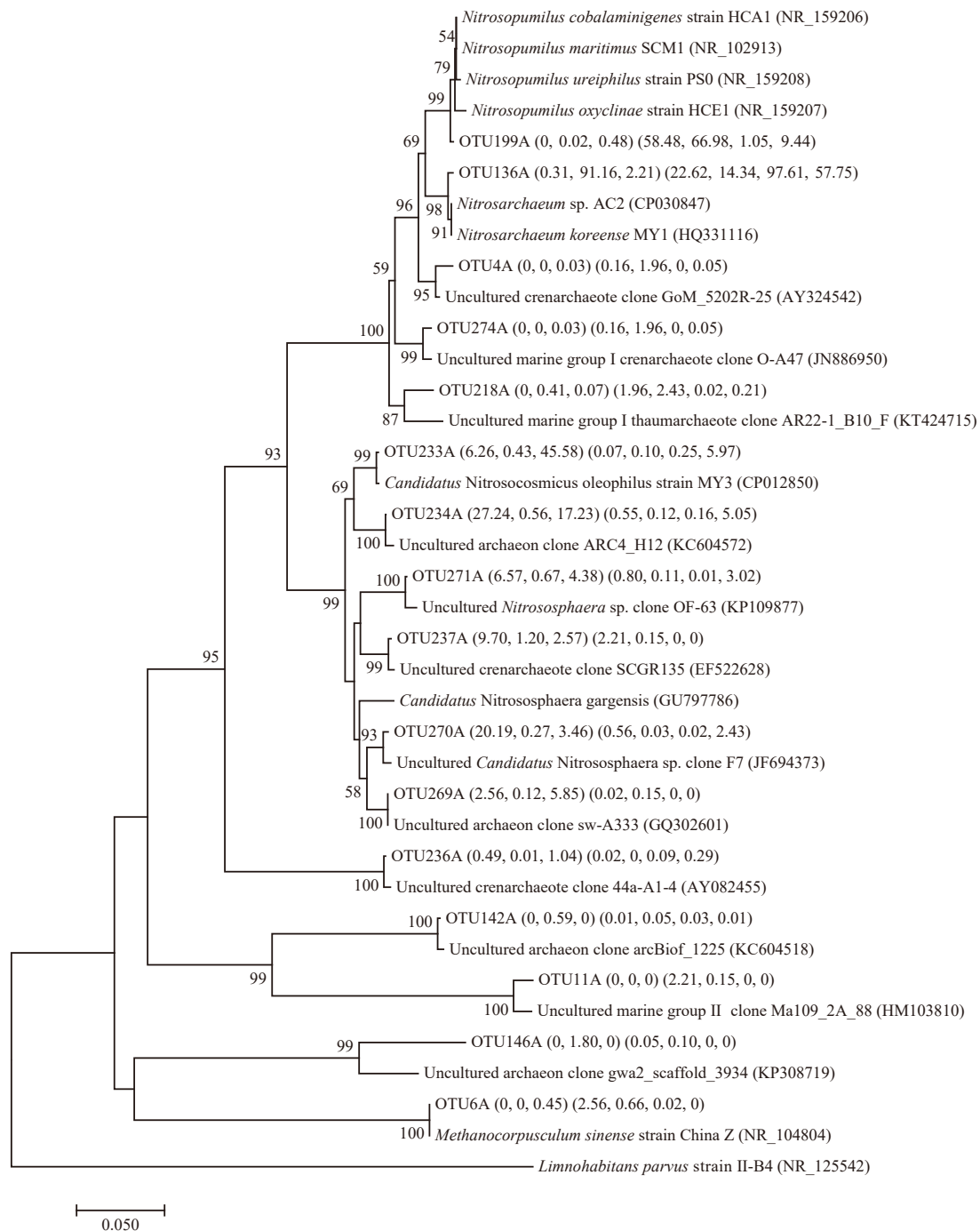


Fig. 6. Neighbor-joining tree showing phylogenetic relationships among the major archaeal operational taxonomic units (OTUs) and reference 16S rRNA gene sequences retrieved from the National Center for Biotechnology Information (NCBI) GenBank. These OTUs were those that ranked top five reads from at least a single sample. The scale bar represents the estimated number of nucleotide changes per sequence position. Percentage on nodes refer to the percentage of recovery from 1 000 bootstrap resamplings. Only values larger than 50% are shown. The numbers in parentheses indicate the percentage composition of reads in each station in the following order: (SW1, SW2, SW3) (GW1, GW2, GW3, GW4).

similarity with *Nitrosopumilus cobalaminigenes* strain HCA1 (NR_159206) (Qin et al., 2017), *N. maritimus* SCM1 (NR_102913) (Walker et al., 2010), *N. ureiphilus* strain PS0 (NR_15920) (Qin et al., 2017) and *N. oxycliniae* strain HCE1 (NR_159207) (Walker et al., 2010), which belong to marine ammonia-oxidizing archaea. For example, *N. maritimus* performs a far unrecognized pathway of ammonia conversion to N_2 when oxygen is depleted (Kraft et al., 2022; Martens-Habbenha and Qin, 2022). OTU136A, also known as the ammonia-oxidizing archaea sequence, was found in both groundwater (proportion of OTUs: 14.3%–97.6%) and surface water (proportion of OTUs: 0.3%–91.2%), which had 99.6% match to *Nitrosarchaeum* sp. AC2 (CP030847). In addition, the sequences of OTU233A, OTU234A and OTU270A were obtained from surface water (proportion of OTUs: 0.3%–45.6%) but relatively few in groundwater (proportion of OTUs: 0–6.0%). These sequences exhibited 95.8%–97.1% similarity with *N. viennensis* strain EN76 (NR_134_097) (Stieglmeier et al., 2014), which is also considered as an aerobic and mesophilic, ammonia-oxidizing archaea. Although archaeal analysis was mainly dominated by ammonia-oxidizing process, different strains showed obvious site selectivity, suggesting that high spatial heterogeneity of dominant archaeal species occurred in groundwater-surface water interaction (Ruiz-González et al., 2022).

Therefore, these main species can utilize excess nutrients (e.g., nitrate and ammonia) at groundwater-surface water interface and reduce the amounts of nutrients entering the ocean, thereby affecting the ecological function of the interface by changing the biomass and community structure of the phytoplankton (Chen et al., 2018a; Torre et al., 2019). The utilization of nutrients by these bacteria and archaea communities seems to match the oligonutrients in the Krka River Estuary (Liu et al., 2019). Note that although nutrients can be utilized by microorganisms in STEs, significant input of point-source nutrients may still lead to water quality degradation. For example, large nutrient discharge with high N/P molar ratios (190–320) from Litno Cave (i.e., Station GW1) likely trigger and sustain red tide outbreaks (i.e., Station SW3) (Chen et al., 2020a).

3.4 Connection between microbial community and hydrochemical environment

Hydrochemical parameters such as salinity, temperature and nutrients have commonly been identified as potential environmental drivers of the observed compositional variations in microbial communities at coastal groundwater-surface water inter-

face (Ye et al., 2016; Chen et al., 2020b; Ruiz-González et al., 2022; Yang et al., 2022). We used CCA analysis (Fig. 7) to determine the interaction between microbial communities and hydrochemical environment, and to clarify which environmental factors govern the bacterial and archaeal communities, respectively.

In the current study, CCA analysis revealed that salinity and nutrients (including nitrate, nitrite, ammonia and phosphate) were correlated with the changes of bacterial and archaeal communities (Fig. 7), and in agreement with previous studies in STEs (Ye et al., 2016; Adyasari et al., 2019; Chen et al., 2020b; Ruiz-González et al., 2022). Salinity and nutrient variations may affect microbial metabolism, thus affecting the life-sustaining activities and abundance of microbial communities (Santoro et al., 2006; Xie et al., 2018; Wang et al., 2020; Ruiz-González et al., 2022). In the bacterial analysis, although there were algal bloom outbreaks at both Stations SW1 and SW3, the bacterial communities at Station SW1 were associated with high nutrient concentrations, while a positive association was found between the bacterial communities and salinity at Station SW3 (Fig. 7a). However, salinity and nitrite (a nitrogen cycle intermediate) had a positive association with the archaeal communities at both Stations SW1 and SW3 (Fig. 7b). The results not only indicate that salinity and nutrients play critical roles in the distributions of bacterial and archaeal communities, but also further indicate that variable environmental factors may drive the heterogeneity of bacterial and archaeal communities.

3.5 Ecological implication of microbial community in STEs

SGD has been recognized as one of the most significant pathways for terrestrial dissolved solutes such as nutrients and carbon entry into coastal waters (Santos et al., 2021), but the nature and magnitude of SGD-derived solute inputs depend largely on microbial-dominated biogeochemical transformations in STEs (Ruiz-González et al., 2022). The distribution patterns of microbial communities were closely related to hydrological, geochemical and environmental characteristics in STEs (Fig. 8). Previous studies (including our study site) have shown that the significant changes of nutrients or salinity associated with SGD could result in variations in the phytoplankton biomass or ecological impairments such as hypoxia, eutrophication or algal bloom (Lecher and Mackey, 2018; Adolf et al., 2019; Chen et al., 2020a; Guo et al., 2020; Zhao et al., 2021), which are adding its share of pressure on the coastal zone and increasing pressure on these coastal resources, especially in mariculture regions (Wang et al., 2021; Yu

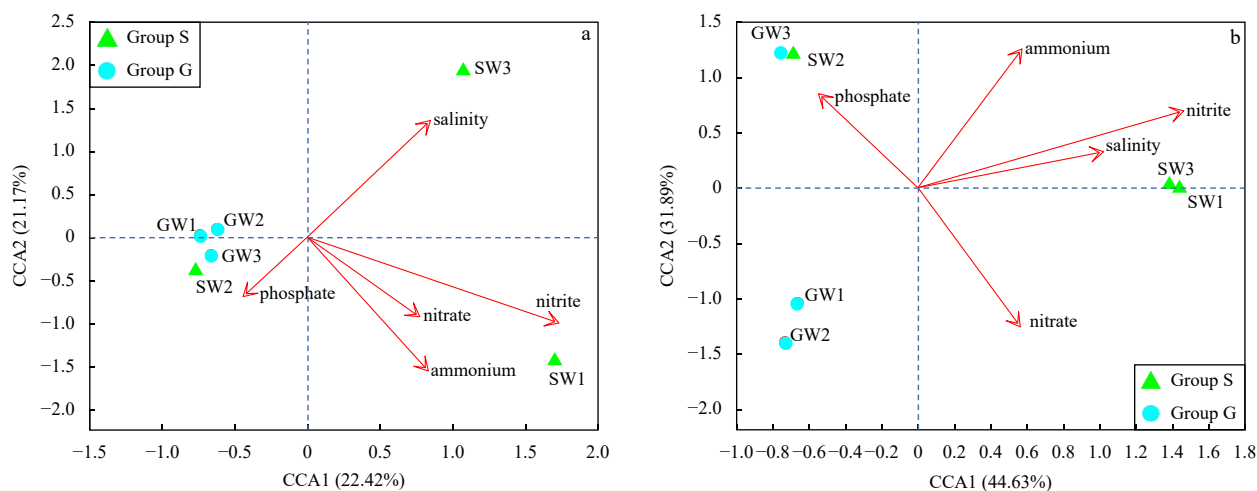


Fig. 7. Canonical correspondence analysis (CCA) analysis showing the bacterial (a) and archaeal (b) community compositions in relation to environmental characteristics. The values of axes 1 and 2 are the percentages explained by the corresponding axis.

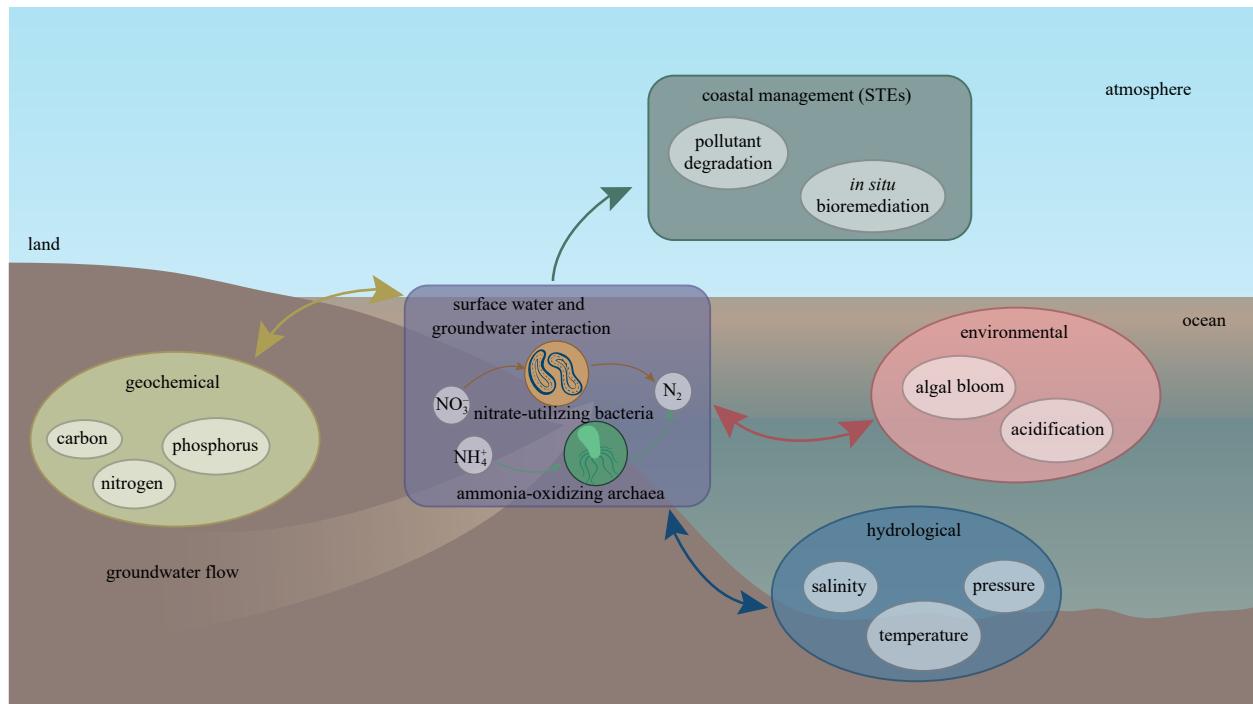


Fig. 8. A conceptual model illustrating interaction between microbial community patterns and hydrological, geochemical and environmental characteristics in karstic subterranean estuaries (STEs).

et al., 2022).

In the present work, we found that some of the bacterial sequences were related to cultured isolates (e.g., *Simplicispira* sp., *Novosphingobium* sp., *Pseudorhodobacter* sp., *Marivivens* sp. and *Aquirufa* sp.), and archaeal sequences were close to ammonia-

oxidizing archaea (e.g., *Nitrosopumilus* spp. and *Nitrosarchaeum* sp.). These microbes could significantly and effectively participate in the removal of groundwater pollutants such as nitrate or ammonia (Table 3). Not only in karstic STEs, several previous studies have also found that microorganisms can significantly

Table 3. A summary of the case study for *in situ* degradation of coastal groundwater pollutants

| Study site | Country | Ecosystem type | Key bacteria | Key archaea | <i>In situ</i> degradation of pollutants | References |
|--------------------|-----------|-----------------------|---|--|--|------------------------|
| Huntington Beach | USA | beach | nitrite reductase-encoding gene fragments (<i>nirK</i> and <i>nirS</i>) | NA | denitrification | Santoro et al. (2006) |
| Huntington Beach | USA | beach | <i>Betaproteobacterial</i> ammonia-oxidizing bacteria | ammonia-oxidizing archaea | nitrogen removal | Santoro et al. (2008) |
| Yellow Sea | China | marginal sea | <i>Comamonas</i> spp. | NA | degrading aromatic compounds | Ye et al. (2016) |
| Northern Java | Indonesia | beach | <i>Burkholderiaceae</i> , <i>Limnohabitans</i> , <i>Flavobacterium</i> , <i>Novosphingobium</i> , <i>Acidovorax</i> , and <i>Sediminibacterium</i> | NA | performing nitrification and denitrification | Adyasari et al. (2019) |
| Qinzhou Bay | China | bay | <i>Gallionella</i> spp., <i>Limnohabitans</i> spp., and <i>Novosphingobium</i> spp. | <i>Bathyarchaeota</i> | utilization of dissolved organic matter; degradation of aromatic compounds | Chen et al. (2019) |
| Shengsi Island | China | volcanic island/beach | <i>Erythrobacter citreu</i> , <i>Halomonas zhaodongensi</i> , <i>Marivivens donghaensi</i> , <i>Pelagibacterium nitratireducen</i> , <i>Novosphingobium naphtha</i> , <i>Pseudomonas pseudoalcaligene</i> , and <i>Nevskia ramosa</i> | NA | utilization of nitrate and organic pollutants | Chen et al. (2020b) |
| Sanggou Bay | China | bay/beach | <i>Pseudoalteromonas</i> | <i>Nitrosopumilus</i> spp. | degradation of refractory sediment organic carbon and ammonia removal | Jiang et al. (2020) |
| Pargos | Mexico | submarine spring | <i>Campylobacteria</i> | NA | nitrate reduction | Huang et al. (2021) |
| Krka River Estuary | Croatia | estuary | <i>Simplicispira</i> sp., <i>Novosphingobium</i> sp., <i>Pseudorhodobacter</i> sp., <i>Marivivens</i> sp., <i>Aquirufa</i> sp. | <i>Nitrosopumilus</i> spp. <i>Nitrosarchaeum</i> sp. | nitrate and ammonia removal | this study |

Note: NA represents no data.

degrade pollutants in different STEs such as estuary, bay, sandy beach, submarine spring, volcanic island and marginal sea before they are discharged into coastal waters (Ye et al., 2016; Adyasari et al., 2019; Chen et al., 2019, 2020b; Jiang et al., 2020; Huang et al., 2021) (Table 3). For example, *Limnohabitans*, *Novosphingobium*, *Marivivens* and *Nitrosopumilus* are widely distributed in different STEs, which can significantly remove the nitrate, ammonia and organic pollutants in coastal groundwater. Therefore, these potential key species likely play important ecological roles in the *in situ* degradation of terrestrial pollutants in STEs (Fig. 8), which can be selected as excellent candidates for bioremediation of polluted groundwater, especially coastal saline groundwater.

4 Conclusions

In this study, we provided perspective into the correlations and heterogeneity of representative microbial taxonomic groups and related ecological functions in groundwater-surface water interaction. The nutrients and salinity were the primary factors in determining the diversity and distribution of microbial communities. Taxonomic composition suggests that the key microbial communities, such as *Simplicispira* sp., *Novosphingobium* sp., *Pseudorhodobacter* sp., *Marivivens* sp., *Aquirufa* sp., *Nitrosopumilus* spp. and *Nitrosarchaeum* sp., can effectively remove the nitrate and ammonia at groundwater-surface water interface in the Krka River Estuary, which can provide a new perspective for coastal groundwater management such as *in situ* degradation/remediation of pollutants in STEs. As STEs are affected by high intensity human activities such as nutrient pollution, this study is essential to understanding the linkages between the distribution patterns of microbial communities and hydrological, geochemical and environmental characteristics in STEs.

References

- Adolf J E, Burns J, Walker J K, et al. 2019. Near shore distributions of phytoplankton and bacteria in relation to submarine groundwater discharge-fed fishponds, Kona coast, Hawai'i, USA. *Estuarine, Coastal and Shelf Science*, 219: 341–353, doi: [10.1016/j.ecss.2019.01.021](https://doi.org/10.1016/j.ecss.2019.01.021)
- Adyasari D, Hassenrück C, Montiel D, et al. 2020. Microbial community composition across a coastal hydrological system affected by submarine groundwater discharge (SGD). *PLoS ONE*, 15(6): e0235235, doi: [10.1371/journal.pone.0235235](https://doi.org/10.1371/journal.pone.0235235)
- Adyasari D, Hassenrück C, Oehler T, et al. 2019. Microbial community structure associated with submarine groundwater discharge in northern Java (Indonesia). *Science of the Total Environment*, 689: 590–601, doi: [10.1016/j.scitotenv.2019.06.193](https://doi.org/10.1016/j.scitotenv.2019.06.193)
- Altschul S F, Madden T L, Schäffer A A, et al. 1997. Gapped BLAST and PSI-BLAST: a new generation of protein database search programs. *Nucleic Acids Research*, 25(17): 3389–3402, doi: [10.1093/nar/25.17.3389](https://doi.org/10.1093/nar/25.17.3389)
- Archana A, Francis C A, Boehm A B. 2021. The beach aquifer microbiome: research gaps and data needs. *Frontiers in Environmental Science*, 9: 653568, doi: [10.3389/fenvs.2021.653568](https://doi.org/10.3389/fenvs.2021.653568)
- Bishop R E, Humphreys W F, Cukrov N, et al. 2015. 'Anchialine' redefined as a subterranean estuary in a crevicular or cavernous geological setting. *Journal of Crustacean Biology*, 35(4): 511–514, doi: [10.1163/1937240X-00002335](https://doi.org/10.1163/1937240X-00002335)
- Boehm A B, Shellenbarger G G, Paytan A. 2004. Groundwater discharge: potential association with fecal indicator bacteria in the surf zone. *Environmental Science & Technology*, 38(13): 3558–3566, doi: [10.1021/es035385a](https://doi.org/10.1021/es035385a)
- Bonacci O, Jukić D, Ljubenkov I. 2006. Definition of catchment area in karst: case of the rivers Krčić and Krka, Croatia. *Hydrological Sciences Journal*, 51(4): 682–699, doi: [10.1623/hysj.51.4.682](https://doi.org/10.1623/hysj.51.4.682)
- Cai Pinghe, Shi Xiangming, Hong Qingquan, et al. 2015. Using $^{224}\text{Ra}/^{228}\text{Th}$ disequilibrium to quantify benthic fluxes of dissolved inorganic carbon and nutrients into the Pearl River Estuary. *Geochimica et Cosmochimica Acta*, 170: 188–203, doi: [10.1016/j.gca.2015.08.015](https://doi.org/10.1016/j.gca.2015.08.015)
- Caporaso J G, Kuczynski J, Stombaugh J, et al. 2010. QIIME allows analysis of high-throughput community sequencing data. *Nature Methods*, 7(5): 335–336, doi: [10.1038/nmeth.f.303](https://doi.org/10.1038/nmeth.f.303)
- Cardenas M B, Rodolfo R S, Lapus M R, et al. 2020. Submarine groundwater and vent discharge in a volcanic area associated with coastal acidification. *Geophysical Research Letters*, 47(1): e2019GL085730, doi: [10.1029/2019GL085730](https://doi.org/10.1029/2019GL085730)
- Chaudhary D K, Kim J. 2016. *Novosphingobium naphthae* sp. nov., from oil-contaminated soil. *International Journal of Systematic and Evolutionary Microbiology*, 66(8): 3170–3176, doi: [10.1099/ijsem.0.001164](https://doi.org/10.1099/ijsem.0.001164)
- Chen Xiaogang, Cukrov N, Santos I R, et al. 2020a. Karstic submarine groundwater discharge into the Mediterranean: radon-based nutrient fluxes in an anchialine cave and a basin-wide upscaling. *Geochimica et Cosmochimica Acta*, 268: 467–484, doi: [10.1016/j.gca.2019.08.019](https://doi.org/10.1016/j.gca.2019.08.019)
- Chen Xiaogang, Du Jinzhou, Yu Xueqing, et al. 2021a. Porewater-derived dissolved inorganic carbon and nutrient fluxes in a salt-marsh of the Changjiang River Estuary. *Acta Oceanologica Sinica*, 40(8): 32–43, doi: [10.1007/s13131-021-1797-z](https://doi.org/10.1007/s13131-021-1797-z)
- Chen Xiaogang, Lao Yanling, Wang Jinlong, et al. 2018a. Submarine groundwater-borne nutrients in a tropical bay (Maowei Sea, China) and their impacts on the oyster aquaculture. *Geochemistry, Geophysics, Geosystems*, 19(3): 932–951, doi: [10.1002/2017GC007330](https://doi.org/10.1002/2017GC007330)
- Chen Xiaogang, Santos I R, Call M, et al. 2021b. The mangrove CO₂ pump: tidally driven pore-water exchange. *Limnology and Oceanography*, 66(4): 1563–1577, doi: [10.1002/lno.11704](https://doi.org/10.1002/lno.11704)
- Chen Xiaogang, Santos I R, Hu Duofei, et al. 2022. Pore-water exchange flushes blue carbon from intertidal saltmarsh sediments into the sea. *Limnology and Oceanography Letters*, 7(4): 312–320, doi: [10.1002/lol2.10236](https://doi.org/10.1002/lol2.10236)
- Chen Xiaogang, Ye Qi, Du Jinzhou, et al. 2019. Bacterial and archaeal assemblages from two size fractions in submarine groundwater near an industrial zone. *Water*, 11(6): 1261, doi: [10.3390/w11061261](https://doi.org/10.3390/w11061261)
- Chen Xiaogang, Ye Qi, Sanders C J, et al. 2020b. Bacterial-derived nutrient and carbon source-sink behaviors in a sandy beach subterranean estuary. *Marine Pollution Bulletin*, 160: 111570, doi: [10.1016/j.marpolbul.2020.111570](https://doi.org/10.1016/j.marpolbul.2020.111570)
- Chen Xiaogang, Zhang Fenfen, Lao Yanling, et al. 2018b. Submarine groundwater discharge-derived carbon fluxes in mangroves: an important component of blue carbon budgets?. *Journal of Geophysical Research: Oceans*, 123(9): 6962–6979, doi: [10.1029/2018JC014448](https://doi.org/10.1029/2018JC014448)
- Chen Xiaogang, Zhu Peiyuan, Zhang Yan, et al. 2023. Plum rain enhances porewater greenhouse gas fluxes and weakens the acidification buffering potential in saltmarshes. *Journal of Hydrology*, 616: 128686, doi: [10.1016/j.jhydrol.2022.128686](https://doi.org/10.1016/j.jhydrol.2022.128686)
- DeLong E F, Karl D M. 2005. Genomic perspectives in microbial oceanography. *Nature*, 437(7057): 336–342, doi: [10.1038/nature04157](https://doi.org/10.1038/nature04157)
- Edgar R C. 2013. UPARSE: highly accurate OTU sequences from microbial amplicon reads. *Nature Methods*, 10(10): 996–998, doi: [10.1038/nmeth.2604](https://doi.org/10.1038/nmeth.2604)
- Edgar R C, Haas B J, Clemente J C, et al. 2011. UCHIME improves sensitivity and speed of chimera detection. *Bioinformatics*, 27(16): 2194–2200, doi: [10.1093/bioinformatics/btr381](https://doi.org/10.1093/bioinformatics/btr381)
- Guo Xiaoyi, Xu Bochao, Burnett W C, et al. 2020. Does submarine groundwater discharge contribute to summer hypoxia in the Changjiang (Yangtze) River Estuary?. *Science of the Total Environment*, 719: 137450, doi: [10.1016/j.scitotenv.2020.137450](https://doi.org/10.1016/j.scitotenv.2020.137450)
- Huang Laibin, Bae H S, Young C, et al. 2021. *Campylobacterota* dominate the microbial communities in a tropical karst subterranean estuary, with implications for cycling and export of nitrogen to coastal waters. *Environmental Microbiology*, 23(11):

- 6749–6763, doi: [10.1111/1462-2920.15746](https://doi.org/10.1111/1462-2920.15746)
- Hwang D W, Lee Y W, Kim G. 2005. Large submarine groundwater discharge and benthic eutrophication in Bangdu Bay on volcanic Jeju Island, Korea. *Limnology and Oceanography*, 50(5): 1393–1403, doi: [10.4319/lo.2005.50.5.1393](https://doi.org/10.4319/lo.2005.50.5.1393)
- Jiang Shan, Zhang Yixue, Jin Jie, et al. 2020. Organic carbon in a seepage face of a subterranean estuary: turnover and microbial interrelations. *Science of the Total Environment*, 725: 138220, doi: [10.1016/j.scitotenv.2020.138220](https://doi.org/10.1016/j.scitotenv.2020.138220)
- Kasalický V, Jezbera J, Šimek K, et al. 2010. *Limnohabitans planktonicus* sp. nov. and *Limnohabitans parvus* sp. nov., planktonic *Betaproteobacteria* isolated from a freshwater reservoir, and emended description of the genus *Limnohabitans*. *International Journal of Systematic and Evolutionary Microbiology*, 60(12): 2710–2714, doi: [10.1099/ijs.0.018952-0](https://doi.org/10.1099/ijs.0.018952-0)
- Knee K L, Layton B A, Street J H, et al. 2008. Sources of nutrients and fecal indicator bacteria to nearshore waters on the north shore of Kaua'i (Hawai'i, USA). *Estuaries and Coasts*, 31(4): 607–622, doi: [10.1007/s12237-008-9055-6](https://doi.org/10.1007/s12237-008-9055-6)
- Kraft B, Jehmlich N, Larsen M, et al. 2022. Oxygen and nitrogen production by an ammonia-oxidizing archaeon. *Science*, 375(6576): 97–100, doi: [10.1126/science.abe6733](https://doi.org/10.1126/science.abe6733)
- Kwokál Ž, Cukrov N, Cuculić V. 2014. Natural causes of changes in marine environment: mercury speciation and distribution in anchialine caves. *Estuarine, Coastal and Shelf Science*, 151: 10–20, doi: [10.1016/j.ecss.2014.09.016](https://doi.org/10.1016/j.ecss.2014.09.016)
- Lecher A L, Mackey K R M. 2018. Synthesizing the effects of submarine groundwater discharge on marine biota. *Hydrology*, 5(4): 60, doi: [10.3390/hydrology5040060](https://doi.org/10.3390/hydrology5040060)
- Lee E, Shin D, Hyun S P, et al. 2017. Periodic change in coastal microbial community structure associated with submarine groundwater discharge and tidal fluctuation. *Limnology and Oceanography*, 62(2): 437–451, doi: [10.1002/lno.10433](https://doi.org/10.1002/lno.10433)
- Li Aihua, Liu Hongcan, Hou Weiguo, et al. 2016. *Pseudorhodobacter sinensis* sp. nov. and *Pseudorhodobacter aquaticus* sp. nov., isolated from crater lakes. *International Journal of Systematic and Evolutionary Microbiology*, 66(8): 2819–2824, doi: [10.1099/ijs.0.001061](https://doi.org/10.1099/ijs.0.001061)
- Liu Qian, Charette M A, Henderson P B, et al. 2014. Effect of submarine groundwater discharge on the coastal ocean inorganic carbon cycle. *Limnology and Oceanography*, 59(5): 1529–1554, doi: [10.4319/lo.2014.59.5.1529](https://doi.org/10.4319/lo.2014.59.5.1529)
- Liu Jianan, Hrustić E, Du Jinzhou, et al. 2019. Net submarine groundwater-derived dissolved inorganic nutrients and carbon input to the oligotrophic stratified karstic estuary of the Krka River (Adriatic Sea, Croatia). *Journal of Geophysical Research: Oceans*, 124(6): 4334–4349, doi: [10.1029/2018JC014814](https://doi.org/10.1029/2018JC014814)
- Lu Shipeng, Ryu S H, Chung B S, et al. 2007. *Simplicispira limi* sp. nov., isolated from activated sludge. *International Journal of Systematic and Evolutionary Microbiology*, 57(1): 31–34, doi: [10.1099/ijs.0.64566-0](https://doi.org/10.1099/ijs.0.64566-0)
- Martens-Habbena W, Qin W. 2022. Archaeal nitrification without oxygen. *Science*, 375(6576): 27–28, doi: [10.1126/science.abn0373](https://doi.org/10.1126/science.abn0373)
- Mayfield K K, Eisenhauer A, Ramos D P S, et al. 2021. Groundwater discharge impacts marine isotope budgets of Li, Mg, Ca, Sr, and Ba. *Nature Communications*, 12(1): 148, doi: [10.1038/s41467-020-20248-3](https://doi.org/10.1038/s41467-020-20248-3)
- Moore W S. 1999. The subterranean estuary: a reaction zone of ground water and sea water. *Marine Chemistry*, 65(1–2): 111–125, doi: [10.1016/S0304-4203\(99\)00014-6](https://doi.org/10.1016/S0304-4203(99)00014-6)
- Park S, Kim S, Jung Y T, et al. 2016. *Marivivens donghaensis* gen. nov., sp. nov., isolated from seawater. *International Journal of Systematic and Evolutionary Microbiology*, 66(2): 666–672, doi: [10.1099/ijs.0.000772](https://doi.org/10.1099/ijs.0.000772)
- Pires A C C, Cleary D F R, Almeida A, et al. 2012. Denaturing gradient gel electrophoresis and barcoded pyrosequencing reveal unprecedented archaeal diversity in mangrove sediment and rhizosphere samples. *Applied and Environmental Microbiology*, 78(16): 5520–5528, doi: [10.1128/AEM.00386-12](https://doi.org/10.1128/AEM.00386-12)
- Pitt A, Schmidt J, Koll U, et al. 2019. *Aquirufa antheringensis* gen. nov., sp. nov. and *Aquirufa nivalisilvae* sp. nov., representing a new genus of widespread freshwater bacteria. *International Journal of Systematic and Evolutionary Microbiology*, 69(9): 2739–2749, doi: [10.1099/ijs.0.003554](https://doi.org/10.1099/ijs.0.003554)
- Qin Wei, Heal K R, Ramdasi R, et al. 2017. *Nitrosopumilus maritimus* gen. nov., sp. nov., *Nitrosopumilus cobalaminigenes* sp. nov., *Nitrosopumilus oxycliniae* sp. nov., and *Nitrosopumilus ureiphilus* sp. nov., four marine ammonia-oxidizing archaea of the phylum *Thaumarchaeota*. *International Journal of Systematic and Evolutionary Microbiology*, 67(12): 5067–5079, doi: [10.1099/ijs.0.002416](https://doi.org/10.1099/ijs.0.002416)
- Reading M J, Tait D R, Maher D T, et al. 2021. Submarine groundwater discharge drives nitrous oxide source/sink dynamics in a metropolitan estuary. *Limnology and Oceanography*, 66(5): 1665–1686, doi: [10.1002/lno.11710](https://doi.org/10.1002/lno.11710)
- Rocha C, Robinson C E, Santos I R, et al. 2021. A place for subterranean estuaries in the coastal zone. *Estuarine, Coastal and Shelf Science*, 250: 107167, doi: [10.1016/j.ecss.2021.107167](https://doi.org/10.1016/j.ecss.2021.107167)
- Ruiz-González C, Rodellas V, Garcia-Orellana J. 2021. The microbial dimension of submarine groundwater discharge: current challenges and future directions. *FEMS Microbiology Reviews*, 45(5): fuab010, doi: [10.1093/femsre/fuab010](https://doi.org/10.1093/femsre/fuab010)
- Ruiz-González C, Rodríguez-Pie L, Maister O, et al. 2022. High spatial heterogeneity and low connectivity of bacterial communities along a Mediterranean subterranean estuary. *Molecular Ecology*, 31(22): 5745–5764, doi: [10.1111/mec.16695](https://doi.org/10.1111/mec.16695)
- Santoro A E, Boehm A B, Francis C A. 2006. Denitrifier community composition along a nitrate and salinity gradient in a coastal aquifer. *Applied and Environmental Microbiology*, 72(3): 2102–2109, doi: [10.1128/AEM.72.3.2102-2109.2006](https://doi.org/10.1128/AEM.72.3.2102-2109.2006)
- Santoro A E, Francis C A, De Siewes N R, et al. 2008. Shifts in the relative abundance of ammonia-oxidizing bacteria and archaea across physicochemical gradients in a subterranean estuary. *Environmental Microbiology*, 10(4): 1068–1079, doi: [10.1111/j.1462-2920.2007.01547.x](https://doi.org/10.1111/j.1462-2920.2007.01547.x)
- Santos I R, Chen Xiaogang, Lecher A L, et al. 2021. Submarine groundwater discharge impacts on coastal nutrient biogeochemistry. *Nature Reviews Earth & Environment*, 2(5): 307–323, doi: [10.1038/s43017-021-00152-0](https://doi.org/10.1038/s43017-021-00152-0)
- Schloss P D, Westcott S L, Ryabin T, et al. 2009. Introducing mothur: open-source, platform-independent, community-supported software for describing and comparing microbial communities. *Applied and Environmental Microbiology*, 75(23): 7537–7541, doi: [10.1128/AEM.01541-09](https://doi.org/10.1128/AEM.01541-09)
- Stieglmeier M, Klingl A, Alves R J E, et al. 2014. *Nitrososphaera viennensis* gen. nov., sp. nov., an aerobic and mesophilic, ammonia-oxidizing archaeon from soil and a member of the archaeal phylum *Thaumarchaeota*. *International Journal of Systematic and Evolutionary Microbiology*, 64(8): 2738–2752, doi: [10.1099/ijs.0.063172-0](https://doi.org/10.1099/ijs.0.063172-0)
- Strickland J D H, Parsons T R. 1972. *A Practical Handbook of Seawater Analysis*. 2nd ed. Ottawa: Minister des Approvisionnement et Services, 119–123
- Tamura K, Stecher G, Peterson D, et al. 2013. MEGA6: molecular evolutionary genetics analysis version 6.0. *Molecular Biology and Evolution*, 30(12): 2725–2729, doi: [10.1093/molbev/mst197](https://doi.org/10.1093/molbev/mst197)
- ter Braak C J F. 1986. Canonical correspondence analysis: a new eigenvalue technique for multivariate direct gradient analysis. *Ecology*, 67(5): 1167–1179, doi: [10.2307/1938672](https://doi.org/10.2307/1938672)
- Torre D M, Coyne K J, Kroeger K D, et al. 2019. Phytoplankton community structure response to groundwater-borne nutrients in the Inland Bays, Delaware, USA. *Marine Ecology Progress Series*, 624: 51–63, doi: [10.3354/meps13012](https://doi.org/10.3354/meps13012)
- Walker C B, de la Torre J R, Klotz M G, et al. 2010. *Nitrosopumilus maritimus* genome reveals unique mechanisms for nitrification and autotrophy in globally distributed marine crenarchaea. *Proceedings of the National Academy of Sciences of the United States of America*, 107(19): 8818–8823, doi: [10.1073/pnas.0913533107](https://doi.org/10.1073/pnas.0913533107)
- Wang Guizhi, Jing Wenping, Wang Shuling, et al. 2014. Coastal acidification induced by tidal-driven submarine groundwater dis-

- charge in a coastal coral reef system. *Environmental Science & Technology*, 48(22): 13069–13075, doi: [10.1021/es5026867](https://doi.org/10.1021/es5026867)
- Wang Qianqian, Li Hailong, Zhang Yan, et al. 2019. Evaluations of submarine groundwater discharge and associated heavy metal fluxes in Bohai Bay, China. *Science of the Total Environment*, 695: 133873, doi: [10.1016/j.scitotenv.2019.133873](https://doi.org/10.1016/j.scitotenv.2019.133873)
- Wang Xuejing, Li Hailong, Zheng Chunmiao, et al. 2018. Submarine groundwater discharge as an important nutrient source influencing nutrient structure in coastal water of Daya Bay, China. *Geochimica et Cosmochimica Acta*, 225: 52–65, doi: [10.1016/j.gca.2018.01.029](https://doi.org/10.1016/j.gca.2018.01.029)
- Wang Yongming, Pan Jie, Yang Jun, et al. 2020. Patterns and processes of free-living and particle-associated bacterioplankton and archaeoplankton communities in a subtropical river-bay system in South China. *Limnology and Oceanography*, 65(S1): S161–S179, doi: [10.1002/lno.11314](https://doi.org/10.1002/lno.11314)
- Wang Xilong, Su Kaijun, Chen Xiaogang, et al. 2021. Submarine groundwater discharge-driven nutrient fluxes in a typical mangrove and aquaculture bay of the Beibu Gulf, China. *Marine Pollution Bulletin*, 168: 112500, doi: [10.1016/j.marpolbul.2021.112500](https://doi.org/10.1016/j.marpolbul.2021.112500)
- Wu Jiapeng, Hong Yiguo, Wilson S J, et al. 2021. Microbial nitrogen loss by coupled nitrification to denitrification and anammox in a permeable subterranean estuary at Gloucester Point, Virginia. *Marine Pollution Bulletin*, 168: 112440, doi: [10.1016/j.marpolbul.2021.112440](https://doi.org/10.1016/j.marpolbul.2021.112440)
- Xie Wei, Luo Haiwei, Murugapiran S K, et al. 2018. Localized high abundance of Marine Group II archaea in the subtropical Pearl River Estuary: implications for their niche adaptation. *Environmental Microbiology*, 20(2): 734–754, doi: [10.1111/1462-2920.14004](https://doi.org/10.1111/1462-2920.14004)
- Xiong Jinbo, Liu Yongqin, Lin Xiangui, et al. 2012. Geographic distance and pH drive bacterial distribution in alkaline lake sediments across Tibetan Plateau. *Environmental Microbiology*, 14(9): 2457–2466, doi: [10.1111/j.1462-2920.2012.02799.x](https://doi.org/10.1111/j.1462-2920.2012.02799.x)
- Yang Fan, Liu Sen, Jia Chao, et al. 2022. Identification of groundwater microbial communities and their connection to the hydrochemical environment in southern Laizhou Bay, China. *Environmental Science and Pollution Research*, 29(10): 14263–14278, doi: [10.1007/s11356-021-16812-z](https://doi.org/10.1007/s11356-021-16812-z)
- Yau Y Y Y, Xin Pei, Chen Xiaogang, et al. 2022. Alkalinity export to the ocean is a major carbon sequestration mechanism in a macrotidal saltmarsh. *Limnology and Oceanography*, 67(S2): S158–S170, doi: [10.1002/lno.12155](https://doi.org/10.1002/lno.12155)
- Ye Qi, Liu Jianan, Du Jinzhou, et al. 2016. Bacterial diversity in submarine groundwater along the coasts of the Yellow Sea. *Frontiers in Microbiology*, 6: 1519, doi: [10.3389/fmicb.2015.01519](https://doi.org/10.3389/fmicb.2015.01519)
- Yu Xueqing, Liu Jianan, Chen Xiaogang, et al. 2022. Submarine groundwater-derived inorganic and organic nutrients vs. mariculture discharge and river contributions in a typical mariculture bay. *Journal of Hydrology*, 613: 128342, doi: [10.1016/j.jhydrol.2022.128342](https://doi.org/10.1016/j.jhydrol.2022.128342)
- Zhang Shengdong, Zhao Shibin, Chen Ye, et al. 2021. Effects of submarine groundwater discharge on bacterial community structure in the coastal waters of South Yellow Sea. *Acta Scientiae Circumstantiae (in Chinese)*, 41(12): 4942–4952, doi: [10.13671/j.hjkxxb.2021.0250](https://doi.org/10.13671/j.hjkxxb.2021.0250)
- Zhao Shibin, Xu Bochao, Yao Qinzhen, et al. 2021. Nutrient-rich submarine groundwater discharge fuels the largest green tide in the world. *Science of the Total Environment*, 770: 144845, doi: [10.1016/j.scitotenv.2020.144845](https://doi.org/10.1016/j.scitotenv.2020.144845)
- Zhong Qiangqiang, Puigcorb  V, Chen Xiaogang, et al. 2022. Unexpectedly high dissolved ²¹⁰Pb in coastal groundwaters: is submarine groundwater discharge important in coastal sea?. *Chemical Geology*, 614: 121165, doi: [10.1016/j.chemgeo.2022.121165](https://doi.org/10.1016/j.chemgeo.2022.121165)
- Zhu Peiyuan, Chen Xiaogang, Zhang Yan, et al. 2022. Porewater-derived blue carbon outwelling and greenhouse gas emissions in a subtropical multi-species saltmarsh. *Frontiers in Marine Science*, 9: 884951, doi: [10.3389/fmars.2022.884951](https://doi.org/10.3389/fmars.2022.884951)
- Žic V, Truesdale V W, Cukrov N. 2008. The distribution of iodide and iodate in anchialine cave waters—Evidence for sustained localised oxidation of iodide to iodate in marine water. *Marine Chemistry*, 112(3–4): 168–178, doi: [10.1016/j.marchem.2008.09.001](https://doi.org/10.1016/j.marchem.2008.09.001)